

Title: Rapid visualization of non-melanoma skin cancer

Ethan Walker, Margaret Mann, Kord Honda, Allison Vidimos, Mark Schluchter, Brian Straight, Matthew Bogyo, Daniel Popkin and James P. Basilion

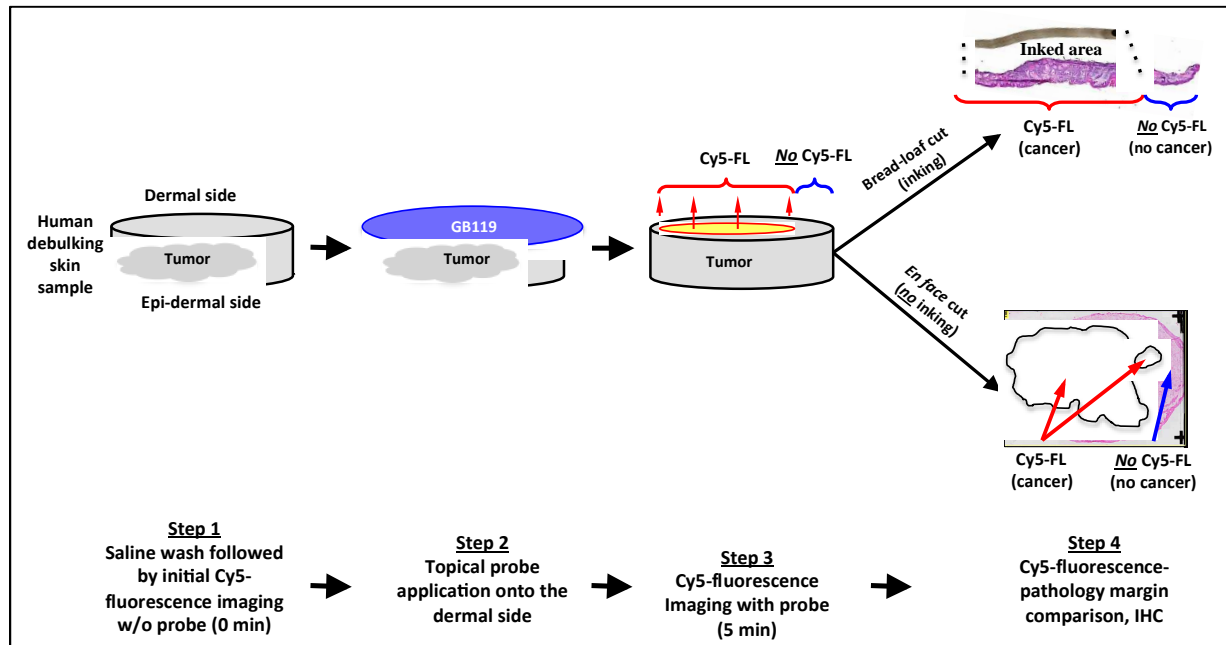
***Corresponding Author:** James P. Basilion, Ph.D.

Professor Departments of Radiology, Biomedical Engineering, and Pathology, Case Center for Imaging Research Case Western Reserve University, Wearn Building, Room B42, 11100 Euclid Ave. Cleveland Ohio, 44106-5056. Email: jxb206@case.edu Tel: 216-983-3264; Fax: 216-844-4987.

List of online-only supplementary materials:

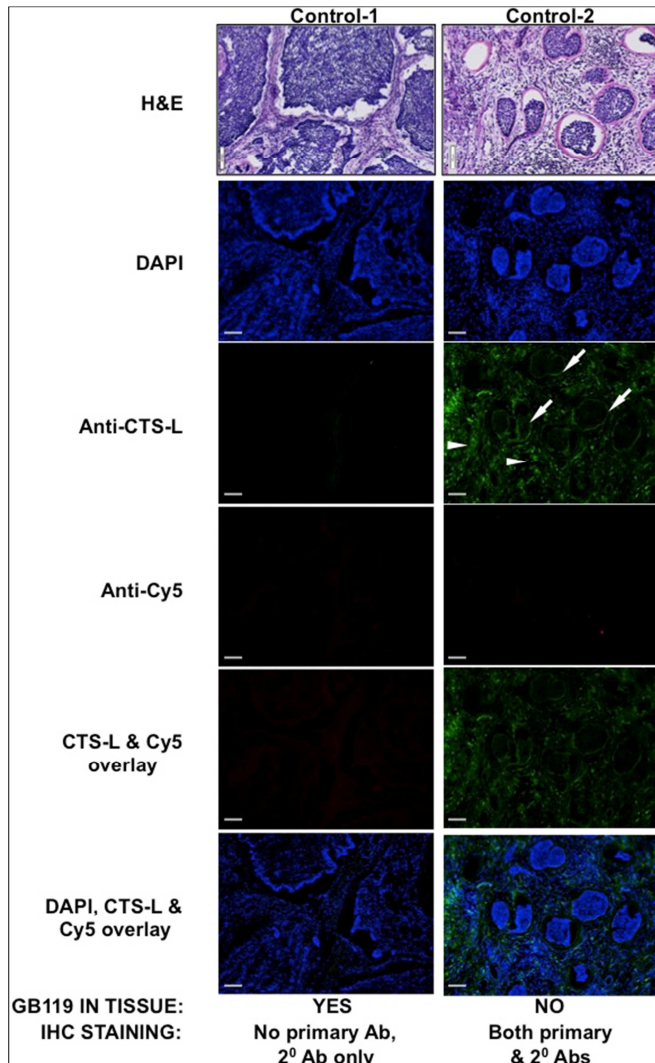
- eFigure 1.** Study design.
- eFigure 2.** IHC controls for detection of probe activation and cathepsin-L expression in BCC containing human skin tissue.
- eFigure 3.** Correlation of pathology throughout the SCC specimen with 2D fluorescence imaging.
- eFigure 4.** Microscopic analysis of regions representing different locations within the sections of SCC sample.
- eFigure 5.** Correlation of probe activation to cancer and cathepsin-B expression in SCC containing human skin tissue.
- eFigure 6.** Effect of blood clots on the 2D fluorescence imaging.
- eFigure 7.** Fold-activation by histopathological diagnosis
- eTable.** Debulking human skin specimen tumor type, tissue depth and fold of activation of GB119.
- eFigure 8.** Assessment of depth of penetration and activation of GB119 in human BCC.
- eFigure 9.** Correlation of pathology throughout the BCC specimen with 2D fluorescence imaging-another example.

eFigure 1 represents the Graphical Abstract.



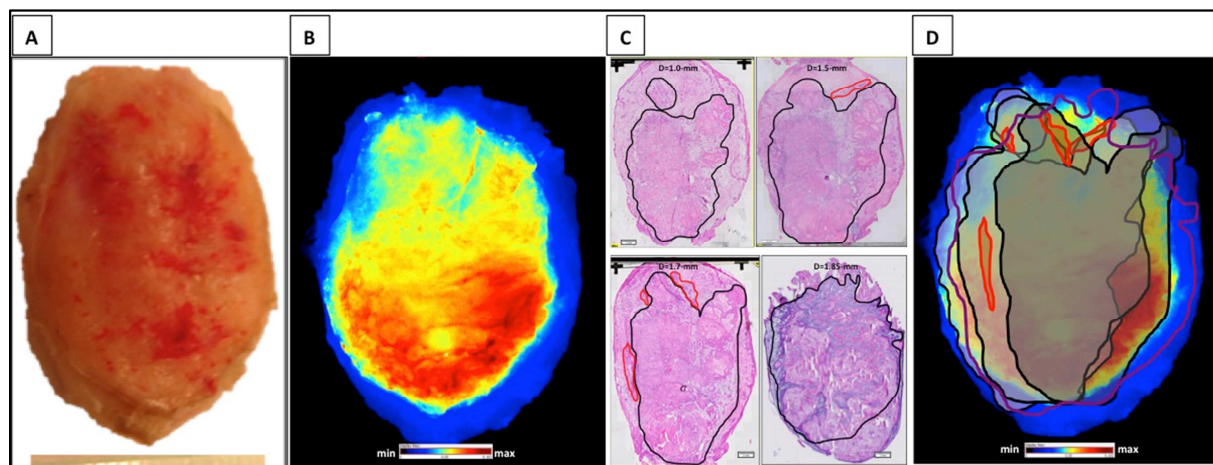
eFigure 1. Study design.

Freshly resected tissues were first washed with sterile saline and then imaged prior to probe application. After initial images (0-min) the probe was applied for 5-min followed by fluorescence imaging (5-min) using the Maestro Imaging System. Samples were then inked to mark fluorescent regions and bread-loaf sectioned or were not inked and underwent *en face* sectioning. Sections underwent H/E staining and then pathologists oriented fluorescent areas with respect to cancer by co-registration with inked areas (bread-loaf sections) or by correlation to cancerous areas (*en face* sections). Bread-loaf data was tabulated and used to determine sensitivity and specificity for detection of the cancer, **Table**.



eFigure 2. IHC controls for detection of probe activation and cathepsin-L expression in BCC containing human skin tissue.

Bread loaf sections of the human skin tissue that was treated with GB119 (Control-1 column) or treated with dimethylsulfoxide as a solvent alone (Control 2 column) and were used to assess the specificity of anti-Cy5 and anti-cathepsin-L antibodies to their target molecules. Control-1 column represents IHC staining of the BCC slides adjacent to H&E slide without primary antibodies. No signal for either cathepsin-L or activated GB119 was detectable. Inclusion of the primary antibody drastically increases signal, see eFigure 4B and **Figure 2B** in the main text. Control-2 column represents IHC staining of the skin tissue that was not pretreated with GB119, i.e. it was Cy5-free, but both primary anti-Cy5 and anti-cathepsin-L antibody as well as secondary antibodies were included. Cathepsin-L is expressed as a zymogen and expression may not correlate with its activity. Increased levels of levels cathepsin-L expression were detected at the edge of BCC “nests” and at the “nest” interface (Control-2), due to inclusion of the primary antibody against cathepsin-L. However, anti-Cy5 antibody was highly specific to its target molecule and never stained BCC “nests” in the GB119-free samples, which were pretreated only with solvent (Control-2). *White arrows* – edges of cancer “nests”; *white arrowheads* – “nest” interface. H&E and IHC scale bars – 100- μ m. Cathepsin-L – false green; nuclei, DAPI – false blue; Cy5, as a part of the probe – false red. One of ten BCC (control-1) and one of four (**Control-2**) representative samples is shown.



eFigure 3. Correlation of pathology throughout the SCC specimen with 2D fluorescence imaging.

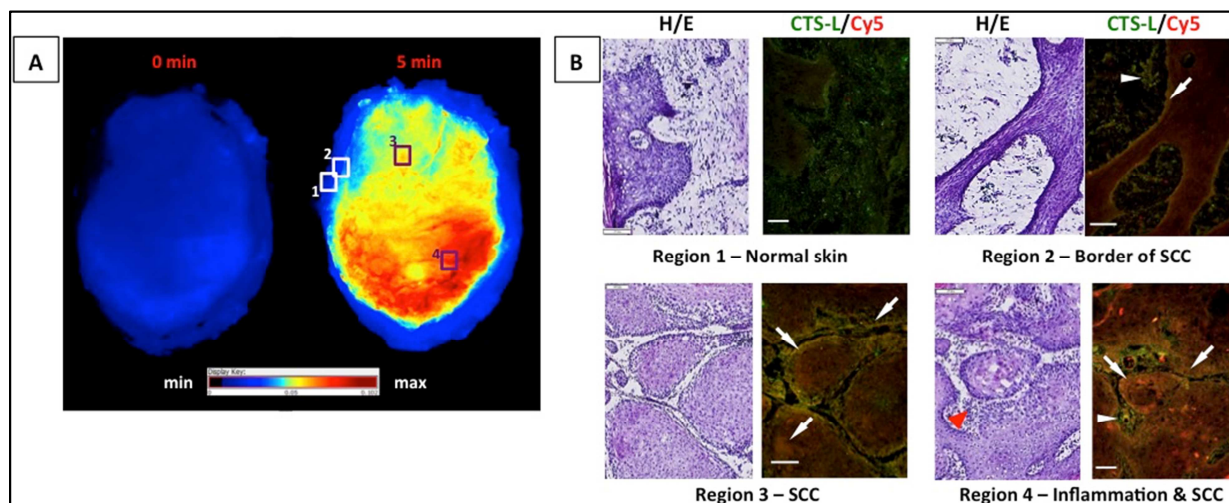
A, Color photo of dermal side of skin sample with a ruler (scale bars – 1-mm).

B, Cy5-fluorescence of skin sample pretreated with GB119. GB119 was topically applied to skin specimens containing cancer. After 5 minutes the sample was imaged using the Maestro imaging device and then frozen *en face* sections was collected.

C, *En face* section histology at different depth. After H/E staining pathologists determined location of the cancer within the section and outlined the cancer with black contour lines. Section depths 1.0-mm, 1.5-mm, 1.7-mm, and 1.85-mm. Scale bars – 2-mm.

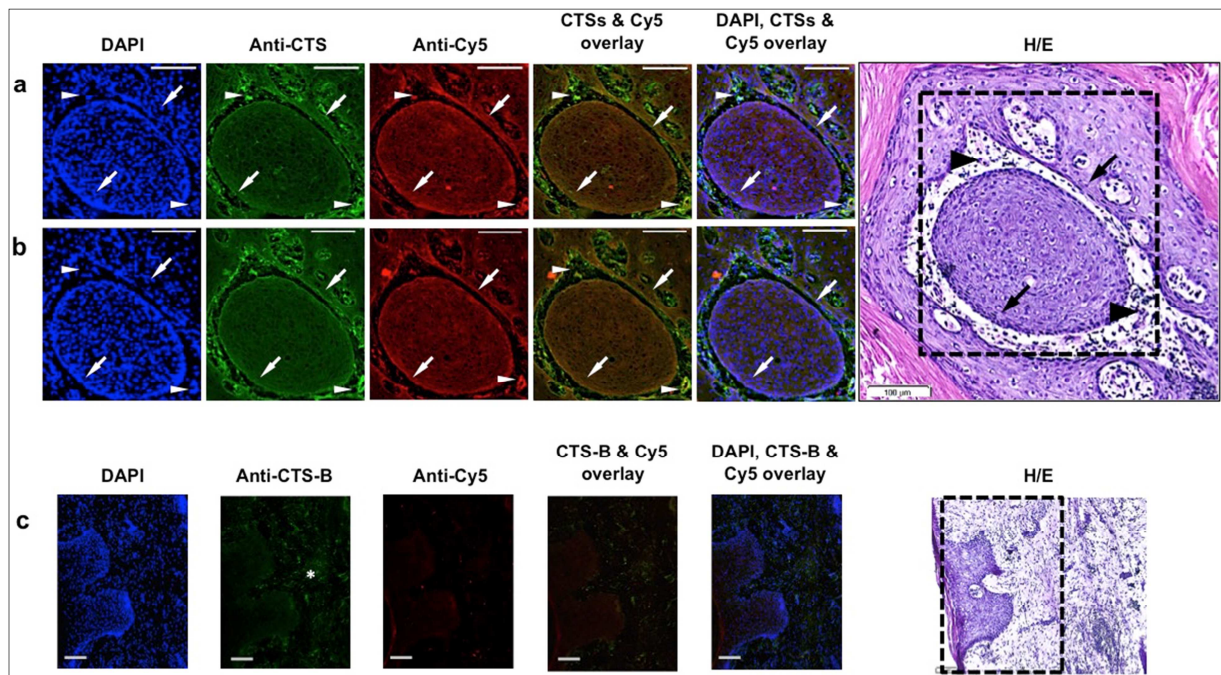
D, Overlay of contours on the 2D-fluorescence image of the skin sample.

The contours were overlaid on the 2D fluorescence image of the skin sample to identify the location of the cancer relative to the fluorescent signal. *Black contours* – cancer perimeter at different depth. *Purple contour* shows SCC area at depth = 1.85-mm. *Red contours* – zones of tissue inflammation. One of three SCC representative samples is shown.



eFigure 4. Microscopic analysis of regions representing different locations within the sections of SCC sample.

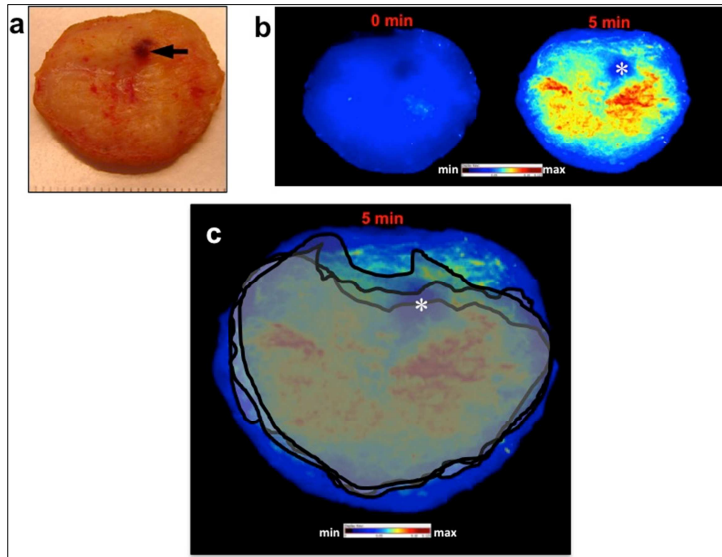
Analysis of SCC specimen in eFigure 3 was used to identify regions of fluorescence for further study. **A**, Cy5-fluorescence of SCC skin specimen pretreated with GB119. Non-fluorescent region (rectangle 1), region bordering fluorescence and non-fluorescent areas (rectangle 2), and areas only within the fluorescent regions (rectangle 3 and 4) were identified for further study. **B**, Co-expression of cathepsin-L and Cy5 in IHC image overlays at different locations of sample. Specimen was subjected to frozen *en face* sectioning followed by H/E and IHC for activated GB119 and cathepsin-L in adjacent sections. *White arrows* – SCC “nests”; *white arrowheads* – SCC “nest” interface. *Orange/brown* color represents co-registration of cathepsin-L and Cy5. *Red arrowhead* – zone of accumulation of inflammatory cells. All scale bars– 100- μ m. One of three SCC representative samples is shown.



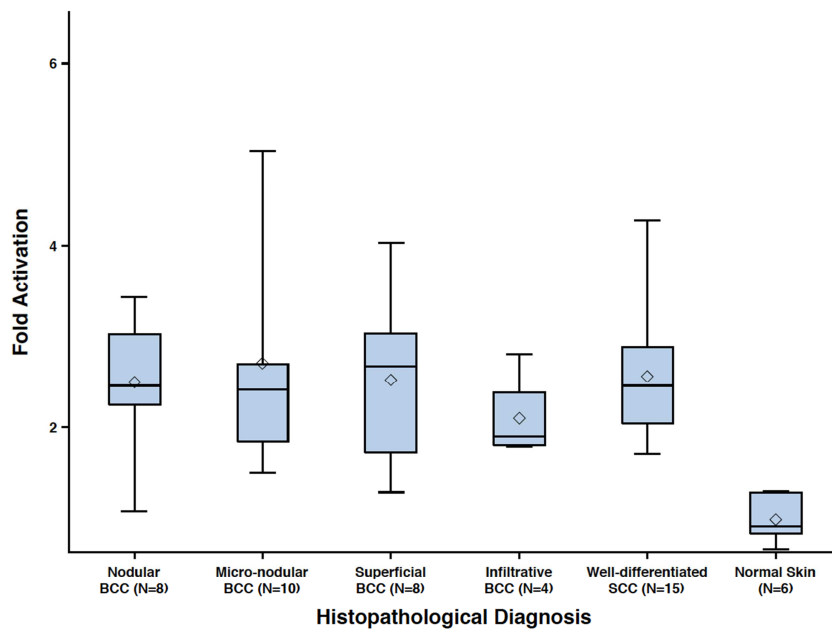
eFigure 5. Correlation of probe activation to cancer and cathepsin-B expression in SCC containing human skin tissue.

En face consecutive sections were used to assess the correlation of probe activation to cancer location and both cathepsin-B and cathepsin-L expression. Anti-cathepsin-B and anti-cathepsin-L antibody demonstrates higher expression of cathepsin-B (a) and cathepsin-L (b) in cancerous tissue (the same location in the sample, see H/E histology at very right) as compared to normal skin tissue (c). Since cathepsin-B and cathepsin-L are expressed as a zymogens and expression may not correlate with activity, we also visualized active probe by staining for activated GB119, column 3 (anti-Cy5). Overlays clearly indicate little to no probe activation in normal tissue (c), but high activation in cancerous tissues (a) and (b). Normal skin tissue expresses cathepsin-B (*white asterisk*) but had little staining for activated GB119. Only cancer tissue shows strong expression of cathepsin-B and -L and strong staining for unquenched/activated probe with good co-registration (*brownish color*). *Arrows* – edges of SCC “nest”; *arrowheads* – “nest” interface. H/E and IHC scale bars – 100- μ m. Cathepsin-B and cathepsin-L – false green; nuclei, DAPI – false blue; Cy5 as a part of the unquenched/activated probe – false red. Two of ten SCC representative samples are shown. Staining for cathepsin-B at the normal tissue (c) represents the same area as in **Figure 4B**, region 1 shown in main text.

eFigure 6. Effect of blood clots on the 2D-fluorescence imaging



This basal cell carcinoma (BCC) skin specimen was treated with GB119, imaged, frozen, and kept at -80°C according to our protocol before histological analysis. (a) Color photos of dermal side of the human BCC skin specimens before the probe application; *black arrow* – pre-formed dense blood clot; ruler bars = 1-mm. (b) Images of Cy5-fluorescence on dermal side of the samples before (0-min) and after topical application of the probe (5-min, Maestro Imaging System); *white asterisk* – positioning of pre-formed dense blood clot. Note the quenching of signal that occurs in the location of the clot. (c) Contours of BCC lesion from three *en face* pathology sections at depths of 1.0-mm, 1.5-mm, and 1.7-mm overlaid on to the 2D-fluorescence image (see Fig. 3 main text). One of six BCC representative samples is shown.



eFigure 7. Probe fold-activation by histopathological diagnosis

GB119/cathepsin-dependent Cy5-fluorescent signal was normalized to imaging area and fold-activation was calculated by dividing the signal from activated probe (5 mins after treatment) by signal from non-treated (0 min) samples. Fold-activation is displayed by histopathological diagnosis using box plots. The bottom and top of each box, respectively, represent the 25th and 75th percentiles, and the lines outside the box extend to the minimum and maximum value. The horizontal line inside the box and the diamond represent the sample median and mean, respectively. Statistical analysis was performed only on data from subtypes that were derived from 4 or more samples. In a one-way analysis of variance comparing means of log-transformed fold-activations among histological diagnoses with Tukey adjustment for multiple comparisons, activation was significantly lower in normal skin compared to all histologic subtypes (adjusted p-values ≤ 0.01), while there were no statistically significant differences among any of histological diagnostic groups.

eTable. Debulked human skin specimen tumor type and tissue depth.

| Total # | Tumor type | Tissue depth (mm) [†] | Fold-activation of GB119 [‡] |
|---------|--------------|--------------------------------|---------------------------------------|
| 1 | BCC; N, MN* | 3.1-4.9 | 6.13 |
| 2 | BCC; N | 1.5-5.1 | 2.18 |
| 3 | BCC, MN | 3.1-4.3 | 2.70 |
| 4 | BCC; I | 3.1-3.9 | 1.97 |
| 5 | SCC; MD, S** | 3.6-4.1 | 2.45 |
| 6 | SCC; WD | 1.9-2.2 | 2.63 |
| 7 | BCC; MN, S | 1.5-2.1 | 3.32 |
| 8 | BCC; MN | 0.9-1.3 | 2.52 |
| 9 | BCC; I | 1.1-1.8 | 2.80 |
| 10 | BCC; S | 2.1-2.8 | 2.59 |
| 11 | BCC; MN | 1.1-3.9 | 1.84 |
| 12 | BCC; S | 1.3-1.8 | 1.99 |
| 13 | SCC; WD | 0.5-0.8 | 4.16 |
| 14 | BCC, MN | 0.5-0.8 | 5.04 |
| 15 | BCC; MN | 1.1-1.8 | 1.51 |
| 16 | SCC; WD | 0.7-0.8 | 2.11 |
| 17 | SCC; WD | 0.9-1.9 | 2.06 |
| 18 | BCC; N, MN | 1.1-1.6 | 2.62 |
| 19 | BCC; N | 1.1-2.0 | 2.55 |
| 20 | SCC; WD | 0.5-1.0 | 2.45 |
| 21 | BCC, S | 0.3-0.5 | 4.03 |
| 22 | SCC; WD | 1.5-2.5 | 2.56 |
| 23 | SCC; WD | 0.7-2.5 | 2.88 |
| 24 | SCC; WD | 1.5-3.9 | 2.32 |
| 25 | BCC; MN | 2.2-5.5 | 4.40 |
| 26 | BCC; MN | 0.7-1.1 | 2.30 |
| 27 | SCC; WD | 0.5-1.2 | 2.65 |
| 28 | SCC; MD | 1.7-4.5 | 2.07 |
| 29 | SCC; WD | 0.5-0.6 | 1.71 |
| 30 | BCC; S | 0.5-1.2 | 1.46 |
| 31 | BCC; I | 1.9-2.7 | 1.82 |
| 32 | SCC; MD | 0.5-1.5 | 1.96 |
| 33 | SCC; MD | 1.3-1.8 | 2.85 |
| 34 | BCC; S, I | 0.5-1.3 | 2.01 |

eTable. Debulk human skin specimen tumor type and tissue depth (cont'd).

| Total # | Tumor type | Tissue depth (mm) [†] | Fold-activation of GB119 [‡] |
|---------|-------------|--------------------------------|---------------------------------------|
| 35 | BCC, MN | 1.1-2.0 | 1.85 |
| 36 | SCC, WD | 0.4-0.5 | 2.91 |
| 37 | BCC; N, MN | 1.4-2.5 | 2.41 |
| 38 | BCC; MN | 0.5-1.8 | 2.62 |
| 39 | BCC; N | 2.1-3.8 | 2.36 |
| 40 | BCC; S | 3.0-4.2 | 2.75 |
| 41 | SCC; WD | 0.9-1.1 | 4.27 |
| 42 | BCC; MN | 0.4-0.5 | 2.30 |
| 43 | BCC; N | 0.5-1.1 | 2.30 |
| 44 | BCC, N | 0.5-0.9 | 1.07 |
| 45 | BCC; I | 0.8-2.5 | 1.79 |
| 46 | BCC; N | 0.9-1.5 | 3.43 |
| 47 | SCC, WD | 0.5-1.2 | 1.79 |
| 48 | BCC; S | 0.3-0.5 | 3.07 |
| 49 | BCC; S | 0.5-1.0 | 3.00 |
| 50 | SCC; WD, MD | 0.5-1.5 | 2.38 |
| 51 | BCC; N | 0.5-1.0 | 2.62 |
| 52 | SCC; WD | 0.8-1.1 | 1.85 |
| 53 | SCC; WD | 1.5-4.0 | 2.04 |
| 54 | BCC; S | 0.2-0.3 | 1.28 |
| 55 | BCC; N | 1.0-1.3 | 3.43 |
| 56 | SCC; WD, MD | 1.1-3.9 | 1.92 |
| 57 | BCC; MN, I | 0.9-2.4 | 2.20 |
| 58 | BCC; I | 0.8-3.1 | 2.25 |
| 59 | SCC; WD | 0.8-3.9 | 2.25 |
| 60 | BCC; N | 1.0-2.4 | 2.60 |
| 61 | BCC; I | 0.8-3.2 | 2.10 |
| 62 | BCC; S | 0.4-3.3 | 1.97 |
| 63 | BCC; S | 0.4-2.0 | 1.93 |
| 64 | SCC; WD | 1.2-2.3 | 2.11 |

Notes: 1) * – BCC – basal cell carcinoma; N – nodular, MN – micro-nodular, S – superficial, and I – infiltrative form of BCC. 2) ** – SCC – squamous cell carcinoma; WD – well differentiated and MD – mildly differentiated forms of SCC. For BCC and SCC M indicates mixed pathology in the sample. 3) [†] – Tissue depth is represented as a min and max distance between dermal and epidermal edges of the skin tissue on H/E histology slide for each sample. 4) [‡] – Fold activation of GB119 represents GB119/cathepsin-dependent Cy5-fluorescent signal that was normalized to imaging area. Fold-activation was calculated by dividing the signal from activated probe (5-min after treatment) by signal from non-treated (0-min) samples. 5) Bread-loaf and *en face* frozen sections (histology and H/E) were used for specimens 1–55 and 56–64, respectively. Samples from 1 to 55 were used to assess both sensitivity and specificity of the method.

eFigure 8. Assessment of depth of penetration and activation of GB119 in human BCC.

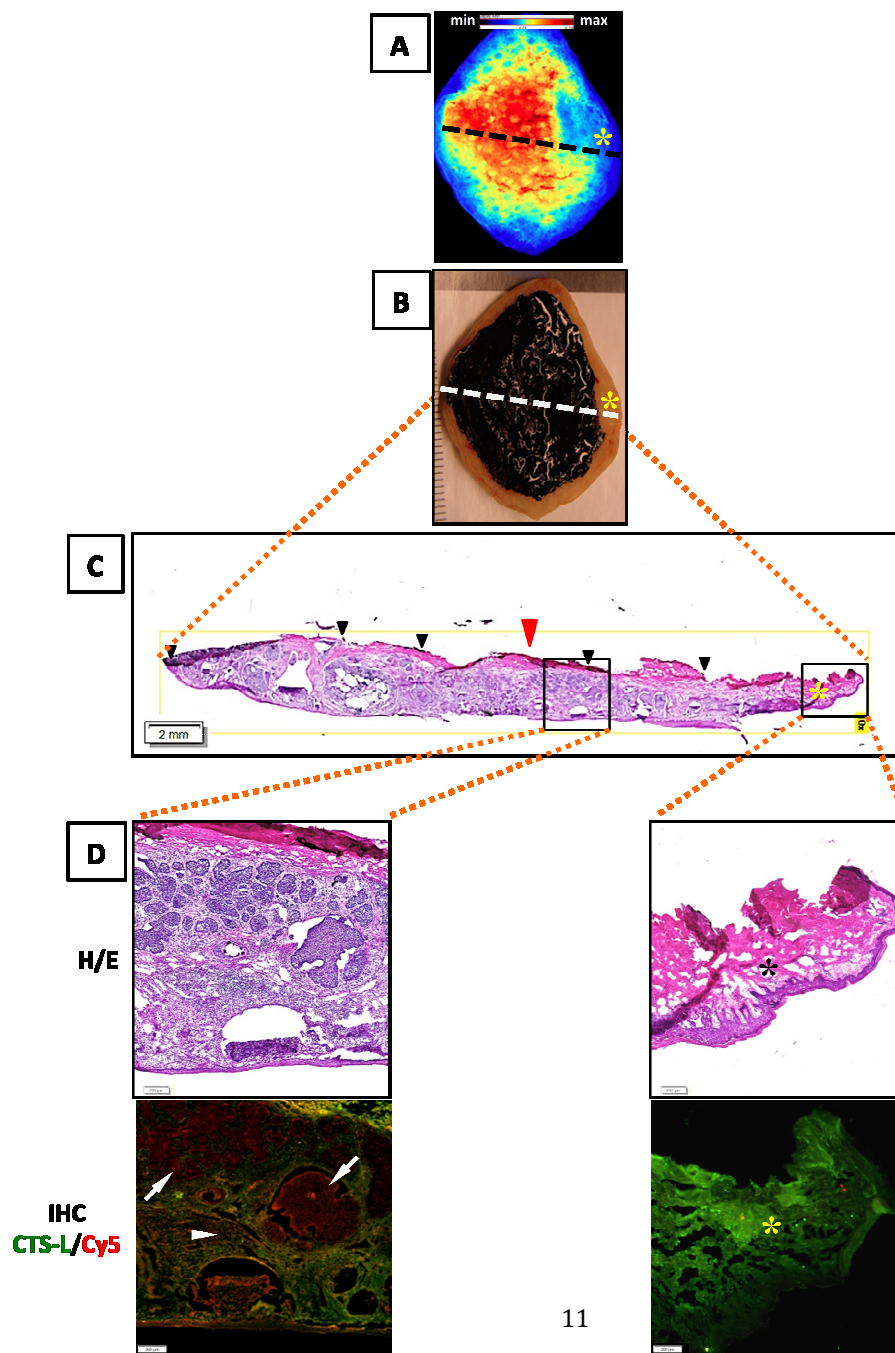
A, Cy5-fluorescent images of dermal side of the human BCC skin specimen after 5-min topical application of GB119. *Dotted line* indicates virtual line of sectioning.

B, Color photo of dermal side of the human BCC skin specimen after inking of fluorescent regions ("hot" spot) in (A).

C, H/E histology image of bread loaf section corresponding to the dotted line in A and B above. *Black arrowheads* indicate the presence of pathology ink demarking fluorescence in fresh sample, A above. *Red arrowhead* indicates surface of application of GB119 (dermal side) and direction of its penetration into the samples.

D, Co-registration of activated probe, cathepsin L and cancerous (left panel) or normal (right panel) tissues. Black arrow heads indicate the location of ink from B locating activation of applied GB119. Overlays show that cathepsin L, probe activation and cancer co-localize throughout the samples, which is 2.5 mm in thickness, left panel. *White arrows* – BCC "nests"; *white arrowhead* – BCC "nest" interface. *Yellow/orange/brown* color represents co-registration, if any, of cathepsin-L and Cy5. The right panel shows that regions of normal skin within the sample do not activate the probe.

Conclusion: Thickness of this particular sample was 2.4-2.5-mm. IHC analysis shows a presence of yellow/orange/brown color in (D) everywhere in the sample indicating presence of activated GB119 all the way through the sample, except in normal tissue.



eFigure 9. Correlation of pathology throughout the BCC specimen with 2D fluorescence imaging-additional example.

A, Cy5-fluorescence of skin sample pretreated with GB119. GB119 was topically applied to the dermal side of skin specimens containing cancer. After 5 minutes the sample was imaged using the Maestro imaging device and then frozen *en face* sections was collected. These sections were derived from the same tissue used to derive figure 3.

B, *En face* section histology at different depths. After H/E staining pathologists determined location of the cancer within the section and outlined the cancer with black contour lines. Section depths 0.2-mm, 0.6-mm, 0.75-mm, 0.85-mm. and 0.9 mm. Scale bars – 2-mm.

D, Overlay of contours on the 2D-fluorescence image of the skin sample.

The contours were overlaid on the 2D fluorescence image of the skin sample to identify the location of the cancer relative to the fluorescent signal. *Black contours* – cancer perimeter at different depth. *Purple contour* shows BCC area at depth = 0.90-mm. *Red contours* – zones of tissue inflammation.

